Resorufin in the Channels of Zeolite L

Dominik Brühwiler, Niklaus Gfeller, and Gion Calzaferri*

Department of Chemistry and Biochemistry, University of Bern, Freiestrasse 3, CH-3000 Bern 9, Switzerland

Received: October 29, 1997

Zeolite L containing the resorufin anion (Res^-) in its anionic framework can be prepared by incorporating the neutral resorufin molecule (ResH) from the gas phase and then exchanging the protons with potassium ions which leads to dark violet colored microcrystals. The reversibility of the deprotonation/protonation reaction of resorufin can be monitored by measuring the UV/vis absorption spectrum of the samples. The absorption spectra of Res^- and ResH and their solvent dependence was interpreted using the EHMO-EDiT theory. While Res^- is strongly fluorescent in solution, the fluorescence is completely quenched when Res^- is located inside the channels of potassium zeolite L. This allows the investigation of the exit kinetics of the resorufin molecules as a function of the size of the solvent molecules which enter the zeolite channels and displace the incorporated resorufin molecules irreversibly. The following series was found for the displacement rate: water $\gg$ methanol > ethanol > 1-propanol $\gtrsim$ 1-butanol. Three cases can be distinguished concerning the mechanism of the displacement process: In case 1 the solvent molecules can pass a dye molecule inside the channel easily. For this case the exit kinetics can be explained by a homogeneous Markoff chain. In case 2 the solvent molecules are considerably hindered when passing a dye molecule inside the channel, and in case 3 the solvent molecules are too large to pass a dye molecule and, hence, the exit rate of dye molecules is zero. While water corresponds to case 1, 1-butanol can be assigned to case 3 and may therefore be used to remove resorufin molecules or molecules with similar properties from the outer surfaces of zeolite L without displacing the intercalated molecules.

Introduction

Zeolites bearing linear channels running through microcrystals offer possibilities to build anisotropic systems with challenging optical,[1−3] electrochemical,[4,5] and photophysical[6−9] properties, and they furthermore allow the investigation of one-dimensional transport processes.[10] While it is well-known that small anions such as Cl^-, Br^-, and I^- can be occluded in the anionic framework of zeolite A by incorporating them from a saturated aqueous alcalihalide solution at elevated temperature[11,12] and while lapis lazuli with its S_3^- radicals as chromophore[13] and analogous synthetic compounds[14] have been studied extensively, no report on anionic organic dye molecules in the channels of zeolite L or of similar structures has been published yet. However, it would be interesting to know if and how such materials can be prepared and what their properties would be. It seems unlikely that the methods which were successfully used for occluding small inorganic ions would work for organic dyes as well. We therefore decided to incorporate a neutral dye molecule which is able to undergo an acid−base reaction. Once inside the channel, the neutral dye molecule can be deprotonated by the addition of a base such as NH_3 or KOR (R = alkyl). The inclusion of the anionic dye molecule would therefore be attained in two steps:

Step 1: Incorporation

$$\text{Zeolite} + \text{DyeH(g)} \rightarrow \text{DyeH(Zeol)}$$

Step 2: Intrazeolite acid base reaction or exchange of cations

$$\text{DyeH(Zeol)} + NH_3\text{(g)} \rightarrow \text{Dye}^-\text{(Zeol)} + NH_4^+\text{(Zeol)}$$

$$\text{DyeH(Zeol)} + \text{KOR(solv)} \rightarrow \text{Dye}^-\text{(Zeol)} + K^+\text{(Zeol)} + \text{ROH}$$

For zeolite L a dye with a similar shape as thionine, of which the exchange isotherm and the spectra were investigated in detail,[15,16] would be preferable. Resorufin (7-hydroxyphenoxazin-3-one) possesses the desired properties and is known to undergo the acid−base reaction illustrated in Scheme 1. The pK_a value for this reaction is 5.5 in water and 6.1 in a 1:1 methanol/water mixture.[17] Note that the molecule gains resonance energy upon dissociation and that charge delocalization causes Res^- to have C_{2v} symmetry. The electronic absorption spectra of the anionic and the neutral form of resorufin are remarkably different; thus, they can be easily distinguished.[18]

Incorporation of ResH into the channels of zeolite L and subsequent deprotonation leads to the Res^-−zeolite L complex shown in Scheme 2, which will allow us to study the displacement of Res^- by different solvent molecules. Furthermore we will show that the electronic absorption spectra of ResH and Res^- in the visible region can be explained by the use of EHMO-EDiT theory.

Experimental Section

Physical Measurements. UV/vis absorption spectra were recorded using a Perkin-Elmer Lambda 14 spectrophotometer. Corrected emission spectra and kinetic measurements were carried out on a Perkin-Elmer LS 50B spectrofluorometer. In both cases 10-mm-path-length quartz cuvettes were used. The integrity of the zeolite samples during different stages of the synthesis was checked by X-ray powder diffraction.

Materials. Zeolite Linde type L with the stoichiometry $K_6Na_3(SiO_2)_{27}(AlO_2)_9 \cdot 21H_2O$ and a particle size of about 0.2 μm was supplied by Union Carbide (ELZ-L). Resorufin was synthesized according to the description of Eichler.[19] Methanol (Merck, pa), ethanol (Merck, abs pa), 1-propanol (Merck, pa), 1-butanol (Dr. Grogg Chemie, purum), acetonitrile (Merck, Uvasol), and pyridine (Merck, Uvasol) were used as received.

Preparation of Resorufin-Loaded Zeolite L. A 4 g amount of zeolite L was suspended in 160 mL of 0.1 M aqueous solution

* Corresponding author. Tel: +41 31 631 4226. E-mail: calza@solar.iac.unibe.ch.

S1089-5647(98)00019-4 CCC: $15.00
Published on Web 03/31/1998

SCHEME 1: Acid−Base Equilibrium of Resorufin

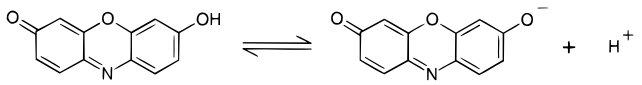

ResH Res⁻

SCHEME 2: Res⁻ Molecule in the Main Channel of Zeolite L

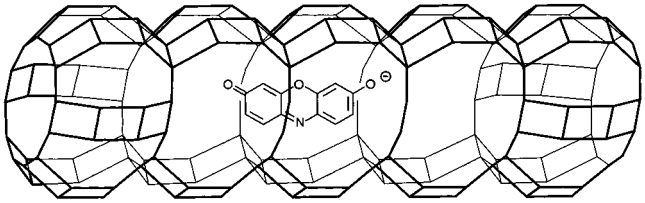

of KCl. After treatment in the supersonic bath the suspension was stirred for 1 h at room temperature. The pH was kept between 8 and 9 by adding small amounts of a 0.1 M aqueous solution of KOH. The zeolite was centrifuged off and dried at 80 °C for 2 h. After grinding the dried zeolite in a mortar, it was activated under vacuum at 350 °C for 6 h and subsequently stored in a drybox to avoid rehydration. A 2 mg amount of ResH was placed in a small glass tube and transferred to the drybox, where 200 mg of activated zeolite was added. The glass tube was evacuated, flame sealed, and then heated to 150 °C for 25 h. The resulting red colored powder was dispersed in 20 mL of ethanol, treated in the supersonic bath, and centrifuged off. After this step was repeated four times, the supernatant solution was colorless and the zeolite samples were orange colored. Since zeolite L exhibits a high affinity toward protons, the supernatant solutions contained only Res^-, as could be shown by measuring their absorption spectra. Because of the high solubility of resorufin in ethanol and the observation that Res^- does not stick to a pure zeolite surface when water or alcohols are used as solvents, we concluded that the remaining adsorbed resorufin molecules were located in the channels of the zeolite and not on its outer surface. The loading of the zeolite with resorufin could be estimated by determining the Res^- concentration of the washing solutions. Loadings of 0.08 resorufin molecules/unit cell of zeolite L were attained by the above procedure. The geometry of zeolite L and the size of the resorufin molecule would allow a highest possible loading of approximately 0.5. Deprotonation of the ResH molecules inside the zeolite could be achieved by the following procedure: 20 mL of 0.2 M ethanolic solution of KOH was added to 200 mg of ResH-loaded zeolite L and shaken at room temperature for 15 min. After centrifugation this step was repeated four times. A continuous change in color of the resorufin loaded zeolite could be observed. The resulting sample was dark violet and showed no fluorescence. During the deprotonation step the loading decreased to 0.07 resorufin molecules/unit cell. After washing with 20 mL of ethanol the samples were stored in 1-butanol.

Kinetic Measurements. A 220 mg sample of Res^--loaded zeolite L was added to 20 mL of 1-butanol and treated in the supersonic bath to give a finely dispersed suspension. A 200 μL volume of the suspension was transferred into a test tube and centrifuged. The supernatant solution was removed carefully, and then 3 mL of the solvent to be investigated was added to the still wet zeolite sample. The resulting suspension was transferred into a quartz cuvette equipped with a magnetic stir bar. The first data point was recorded 1 min after the mixing of the zeolite sample and the solvent. The suspension inside the quartz cuvette was stirred throughout the measurement. In order to get comparable results, the emission was detected at the fluorescence maximum of Res^- in the corresponding solvent with the excitation chosen at 1000 cm^{-1} above the respective maximum. The fluorescence intensity was recorded every 1 min with an integration time of 5 s. After completion of the data acquisition, the suspension was centrifuged and the concentration of Res^- in the supernatant solution was determined, based on which an estimation of the percentage of resorufin molecules displaced by solvent molecules could be made. We define this solvent specific *total displacement* as the amount of displaced resorufin molecules (determined from the concentration of Res^- molecules in solution) divided by the total amount of resorufin molecules in the suspension, which was calculated from the amount of zeolite and its initial loading. Extinction coefficients and absorption and fluorescence maxima of Res^- used for the above procedure are listed in Table 1. For quantitative measurements the initial loading of the zeolite samples was chosen so small that the influences of the inner filter effect and the reabsorption of fluorescence could be neglected.

TABLE 1: Extinction Coefficients, Absorption Maxima, and Fluorescence Maxima of Res^- in Different Solvents

solvent	ϵ_{max} ($L \cdot mol^{-1} \cdot cm^{-1}$)	abs max (nm)	em max (nm)
water	60 000	571	586
methanol	72 000	573	591
ethanol	78 000	578	593
1-propanol	78 000	579	595
1-butanol	78 000	580	596

Theory

Molecular Orbital and Oscillator Strength Calculations. Molecular orbital and oscillator strength calculations were performed using the ICON-EDiT program package,[20] which is based on the extended Hückel molecular orbital (EHMO) method.[21] The off-diagonal elements were calculated as follows:[22]

$$H_{ij} = {}^1/_2 K S_{ij}(H_{ii} + H_{jj}) \tag{1}$$

To determine the Wolfsberg−Helmholz parameter K, a slightly modified distance-dependent form of the weighted formula was used, which is implemented in ICON-EDiT[20] as default.

$$K = 1 + k\left(\frac{\exp(-\delta(R - d_0))}{1 + (\delta(R - d_0 - |R - d_0|))^2}\right) \tag{2}$$

with

$$k = \kappa + \Delta^2 - \Delta^4\kappa \qquad \Delta = \frac{H_{ii} - H_{jj}}{H_{ii} + H_{jj}} \tag{3}$$

H_{ii} and H_{jj} are the Coulomb integrals of the ith and the jth atomic orbital. R is the distance between the atoms on which those atomic orbitals are located. d_0 is the sum of the ith and the jth atomic orbital radii calculated from the corresponding Slater exponents using eqs 13 and 14 in ref 23. To correct for the core−core repulsion, a two-body term as explained in ref 23 has been taken into account. The calculations were carried out with the parameters in Table 2 and the standard parameters $\kappa = 1$ and $\delta = 0.35$ Å^{-1}.

Calculations of the oscillator strength of the electronic dipole-induced transitions based on EHMO wave functions were

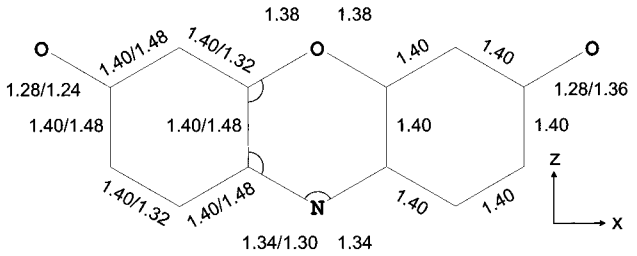

Figure 1. Bond lengths in Å used for the calculation of the influence of protonation on the spectral properties of resorufin. The first number represents the initial bond length as it would appear in a Res^- molecule. The second number corresponds to the bond length after the last transformation step. Bonds with only one given length are assumed to be constant during the transformation. To compensate for the change of bond lengths, the three explicitly drawn angles had to be slightly adjusted. All other angles were kept constant during the transformation. The bond lengths were changed in 8 steps with increments of 0.01 and 0.005 Å, respectively.

TABLE 2: Coulomb Integrals H_{ii} and Slater Exponents ζ Used for EHMO Calculations

element	AO	H_{ii} (eV)	ζ
H	1s	−13.60	1.300
C	2s	−21.40	1.710
	2p	−11.40	1.625
N	2s	−26.00	2.140
	2p	−14.00	1.950
O	2s	−32.30	2.575
	2p	−14.80	2.275

performed using the program EDiT described in ref 24. The protonation process of Res^- on one of the terminal oxygen atoms and its consequences for the spectral properties can be studied by changing the bond lengths to be influenced and monitoring the energy and the oscillator strength of the prominent $\pi^* \leftarrow \pi$ transition. The estimated changes of bond lengths are shown in Figure 1. Calculations were performed at 8 stages during the transformation, which was carried out by modifying the bond lengths in steps of 0.01 and 0.005 Å, respectively. Calculations which include the rotation of the hydroxyl moiety were carried out using the geometry after transformation step 8 and an oxygen−hydrogen bond length of 0.96 Å.

Markoff Chains. The Markoff chain method provides a useful tool for the study of complex processes, such as the growth or decay of populations, without the difficulties of solving differential equations.[25,26] Such an approach was recently used to model the energy migration in dye-loaded hexagonal microporous crystals.[8] The time-dependent irreversible displacement of intercalated resorufin molecules by solvent molecules can be modeled illustratively by the use of this method. In our calculations, the channels of zeolite L are represented by one single channel consisting of 101 sites for resorufin molecules. The length of this channel corresponds well to the length of the channels in commercial zeolite L, when we attribute to each site a length of 15 Å in the *c*-direction. To apply the concept of Markoff chains to the channel of our model system, the sites have to be numbered continuously:

$$k = 0, 1, 2, ..., 100 \quad (4)$$

The sites $k = 0$ and $k = 100$ lie at the ends of the channel; thus, special properties will be attributed to them ($k = 0$ is chosen to be the site at the left end of the channel). We now place a single resorufin molecule inside the channel and assign an occupation probability p_k to each site, thereby considering that at the start of the calculation

$$\sum_{k=0}^{100} p_k = 1 \quad (5)$$

The initial distribution is assumed to be homogeneous; thus all values of p_k will be set equal. The occupation probabilities can be changed by applying a transition matrix **M**. The meaning of the elements m_{ik} of this (101 × 101)-matrix can be described as follows: Elements with $i = k$ represent the probability that the molecule stays on the same site, elements with $i = k - 1$ refer to the probability for a jump to the site on the left (number $k - 1$), and elements with $i = k + 1$ refer to the probability for a jump to the site on the right (number $k + 1$). The absolute values of those probabilities depend on the chosen time interval Δt between two calculation steps. All other elements are set equal to zero, which means that a molecule can only jump to neighboring sites in one calculation step. Note that the properties of a site *k* are listed in the *k*th column of the transition matrix. Since the molecule cannot be lost on a site inside the channel, the elements of a column (except the columns with $k = 0$ and $k = 100$) must fulfil the following equation:

$$\sum_{i=0}^{100} m_{ik} = 1 \quad k = 1, 2, 3, ..., 99 \quad (6)$$

Multiplication of **M** with the vector of the occupation probabilities after *s* calculation steps, **p**(*s*), returns the new occupation probabilities after $s + 1$ calculation steps:

$$\mathbf{p}(s + 1) = \mathbf{M} \cdot \mathbf{p}(s) \quad (7)$$

Results and Discussion

The Resorufin Molecule. The absorption as well as the fluorescence spectrum of resorufin in solution is strongly dependent on the pH (see Figure 2). Protonation of Res^- at one of the terminal oxygen atoms results in a broadening of the absorption and emission spectrum. This is accompanied by a remarkable hypsochromic shift of the absorption band and a loss in vibrational fine structure. However, the absorption band of ResH contains a shoulder at 25 000 cm^{-1} (shown in the insert of Figure 2). Neither the main absorption band nor its shoulder is essentially reduced when heating a solution of ResH in 1-butanol to 95 °C. Since the stability of aggregates decreases with increasing temperature and since there is no essential reduction of oscillator strength upon protonation (the experimentally determined values are 0.9 for ResH and 1.0 for Res^-), we conclude that those bands can be attributed to electronic transitions of monomers of ResH. We will show later that the observations stated above can be explained by EHMO-EDiT theory. The frontier molecular orbitals of Res^- are illustrated in Figure 3. It is obvious that their symmetry and the energy at which they are located allow a relatively simple explanation of the spectra since configuration interaction is negligible in a first-order approximation.

To understand the hypsochromic shift of the prominent $\pi^* \leftarrow \pi$ transition upon protonation, we first have to consider the changes in bond length which are caused by protonation. We will do this first without adding the proton. Figure 4A shows that the magnitude of the spectral shift observed in ResH with respect to Res^- is reproduced quite well. Note that the changes in oscillator strength caused by the alteration of bond lengths are rather small. Let us now consider the influence of the additional proton. This can be done by adding the proton to the distorted resorufin molecule on the appropriate terminal oxygen atom. The loss in symmetry is now obvious when

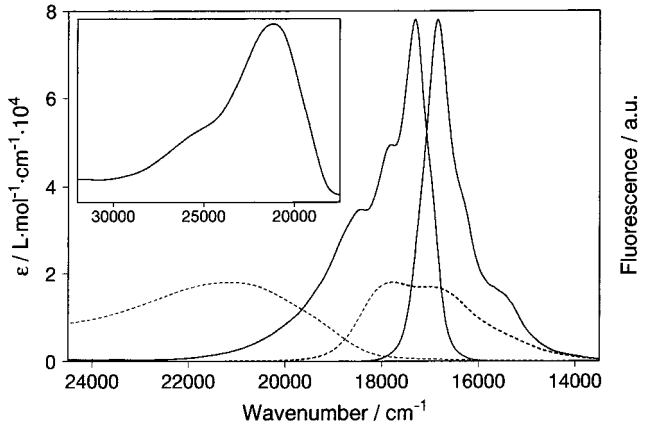

Figure 2. Absorption and fluorescence spectra of Res^- (—) and ResH (---) in ethanol. Excitation was performed at 520 and 450 nm, respectively. The fluorescence spectra have been scaled to the same height as the corresponding absorption spectrum. The insert shows the magnified absorption spectrum of ResH. Note the shoulder at 25 000 cm^{-1}.

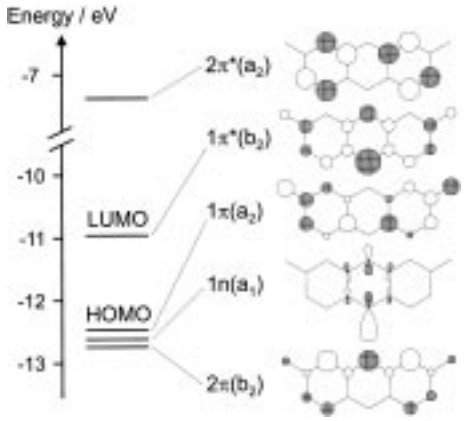

Figure 3. Molecular orbitals in the HOMO−LUMO region of Res^-. (Coefficients smaller than 0.1 are not shown.) Note that the considered one electron states are of different symmetry; thus, no configuration interaction has to be taken into account. The energy of the 1n-orbital will depend strongly on the solvent. The influence of protic and to a smaller extent polar solvents can be simulated by lowering the H_{ii} of the nitrogen 2p-AO.

rotating the hydroxyl moiety, which should be easily possible at room temperature (the calculation gives a rotation barrier of 0.17 eV). This favors orbital mixing which results in a redistribution of oscillator strength. Hence, we will now have to look at not only the prominent $1\pi^* \leftarrow 1\pi$ transition but also at other transitions in the energy range of the broad absorption band of ResH. The calculations give a total of three transitions in this region. First, there is the very intense $1\pi^* \leftarrow 1\pi$ transition which we so far called the prominent transition. As can be seen in Figure 4B, the rotation of the O−H bond out of the molecular plane results in a hypsochromic shift of up to 400 cm^{-1}, which is accompanied by a reduction of oscillator strength. Then there is the $1\pi^* \leftarrow$ 1n transition. Its oscillator strength is very low in any conformation of ResH. More importantly there is the $1\pi^* \leftarrow 2\pi$ transition which seems to be responsible for the shoulder in the ResH absorption band at 25 000 cm^{-1} shown in the insert of Figure 2. The intensity of this transition is increased upon rotation, with a maximum at 90°, while its energy is only slightly shifted (see Figure 5).

The dissimilarity of the absorption spectra of Res^- in different solvents illustrated in Figure 6 can be attributed to variable solvation. Res^- bears high negative partial charges at the terminal oxygen atoms and to a smaller extent on the nitrogen

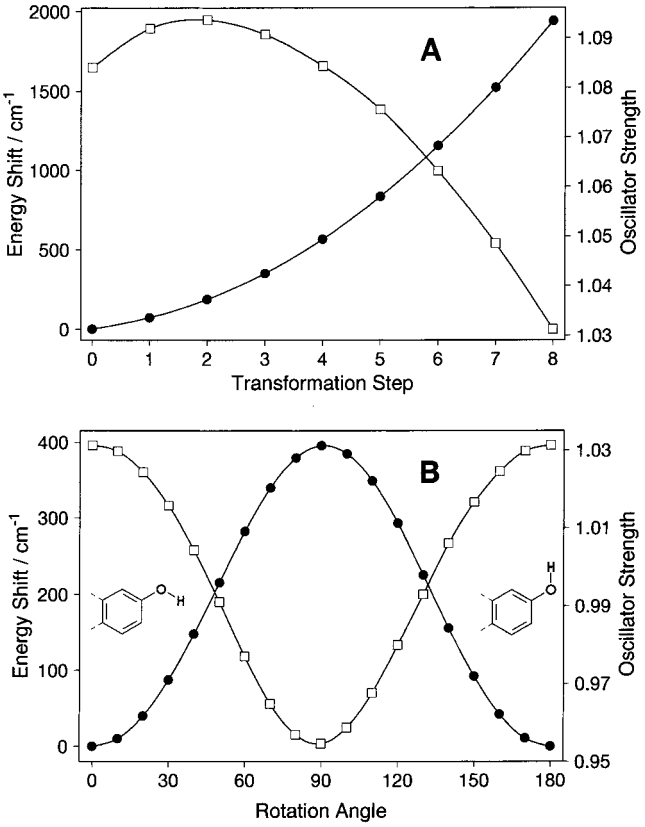

Figure 4. (A) Calculated energy shift (solid circles) and oscillator strength (empty squares) of the $1\pi^* \leftarrow 1\pi$ transition of resorufin upon dependence of the bond lengths (see Figure 1). (B) Calculated energy shift (solid circles) and oscillator strength (empty squares) of the $1\pi^* \leftarrow 1\pi$ transition of resorufin upon dependence of the rotation angle of the oxygen−hydrogen bond.

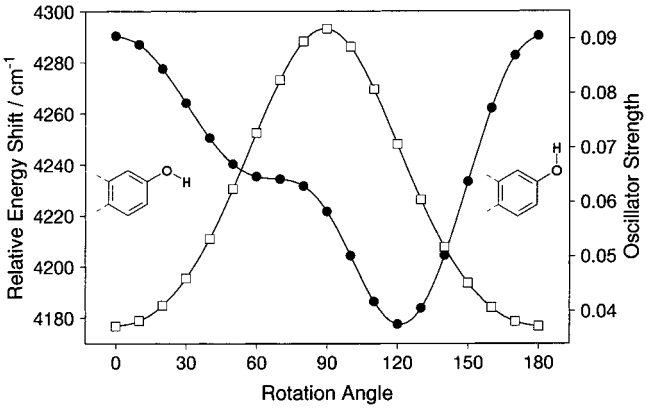

Figure 5. Calculated energy shift (solid circles) of the $1\pi^* \leftarrow 2\pi$ transition relative to the respective energy of the $1\pi^* \leftarrow 1\pi$ transition and oscillator strength (empty squares) of the $1\pi^* \leftarrow 2\pi$ transition upon dependence of the rotation angle of the oxygen−hydrogen bond.

atom. One would therefore expect the formation of strong hydrogen bonds in protic solvents which should influence the electronic absorption spectrum of Res^-. Hydrogen bonds at the terminal oxygen atoms are expected to disturb the symmetry of bonding and charge distribution to some extent. This causes a hypsochromic shift of the $1\pi^* \leftarrow 1\pi$ transition which increases with increasing hydrogen-bonding ability of the solvent. Stronger Res^--solvent interactions also lead to a loss of fine structure. A hydrogen bond at the nitrogen atom, however, causes a bathochromic shift of the $1\pi^* \leftarrow 1\pi$ transition by stabilizing the $1\pi^*$ orbital (see Figure 3). We therefore conclude that the shoulder in the low-energy region of the absorption spectrum

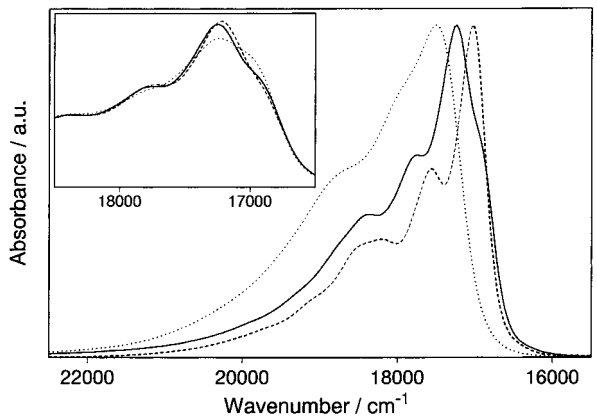

Figure 6. Absorption spectra of Res^- in different solvents: water (···); 1-butanol (—); acetonitrile (- - -). The spectra have been scaled to identical heights. The insert shows the solvent dependence of the shoulder at approximately 17 000 cm^{-1}. Equally concentrated solutions of Res^- in 1-butanol (—), 1-butanol with 5% pyridine (- - -), and 1-butanol with 5% water (···) were used in this case.

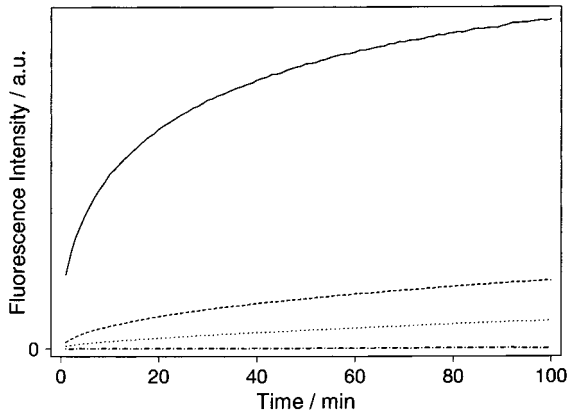

Figure 7. Experimental exit kinetics monitored by the fluorescence intensities of suspensions of Res^--loaded zeolite samples in different solvents: water (—); methanol (- - -); ethanol (···); 1-propanol (— · —). The measurements were started 1 min after the mixing of the suspensions.

of Res^- in 1-butanol corresponds to a species which carries a hydrogen bond at the nitrogen atom. This shoulder is not present in aprotic solvents such as acetonitrile, and it is getting increasingly obscured in the spectra measured in 1-propanol, ethanol, methanol, and water. A further experiment can be done to confirm the conclusions above: Adding pyridine, which is a strong acceptor of hydrogen bonds, to a solution of Res^- in 1-butanol removes the shoulder, and adding water produces the contrary effect (insert in Figure 6). Similar observations have been made by Schellenberg and Friedrich.[27]

Resorufin-Loaded Zeolite L. Samples of Res^--loaded potassium zeolite L can be prepared by incorporating ResH and then exchanging the protons with potassium ions. The absorption spectra of the zeolite samples indicate that this exchange results in a reversible deprotonation of the ResH molecules. Since the absorption spectrum of intercalated Res^- molecules is not shifted to shorter wavelength compared to the spectrum in solution, we assume that the charge delocalization is not significantly reduced when Res^- is incorporated into zeolite L. While Res^- in solution is strongly fluorescent and has even been considered for the use as a laser dye,[28] the fluorescence is quenched when Res^- is located inside the channels of potassium zeolite L. This effect is not yet completely understood, since cationic dye molecules like pyronine and oxonine show strong fluorescence when included into zeolite L.[6−9] However, it is reasonable to assume that the exchangeable cations are involved in the quenching of the Res^- fluorescence. The short distance between the cations and the Res^- molecules, which is enforced by the geometry of the zeolite channel and the electrostatic attraction, as well as the high local concentration of the exchangeable cations (7.2/resorufin site on the average,[29−31] which corresponds to two unit cells) seems to favor fast radiationless deactivation paths for the S_1 state of Res^-.

Exit Kinetics. *Experimental Results.* Figure 7 shows the solvent dependence of the displacement of incorporated resorufin molecules. It is fastest in water and decreases with increasing size of the solvent molecules. There is virtually no displacement in 1-propanol, although a slight increase of fluorescence intensity can be observed compared to the measurement in 1-butanol, which provides the baseline for the experiment. It thereby has to be considered that the solubility of Res^- is similar in the investigated solvents. Since the fluorescence quantum yield increases from water (0.6) to methanol (0.9), the investigated effect is even more distinct than the experiment might suggest.

SCHEME 3: Mechanism of the Displacement of Resorufin Molecules by Solvent Molecules

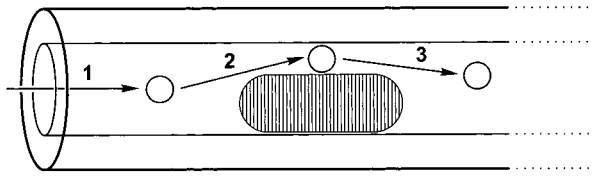

The series

$$\text{water} \gg \text{methanol} > \text{ethanol} > \text{1-propanol} \gtrsim \text{1-butanol}$$

which outlines the ability of solvent molecules to displace intercalated resorufin molecules is independent of the initial loading of the zeolite samples. However, the total displacement after a certain period of time depends on the loading and the quality of the loading of the zeolite samples. The following values for the total displacement after 100 min have been obtained by the procedure described in the Experimental Section: 43% for water, 6% for methanol, 2% for ethanol, and 0% for 1-propanol and 1-butanol. In the case of the alcohols, the zeolite samples retained their dark violet color, but pale orange colored zeolite was obtained after the experiment in water. Apparently the high affinity of the zeolite toward protons lead to the protonation of the incorporated Res^- molecules in the latter case. This did not cause any problems for the measurement, since only Res^- molecules were observed in solution and the exit kinetics did not depend on the Res^-/ResH ratio inside the zeolite channels.

The displacement process in water, although starting very fast, levels off after a certain period of time. Centrifuging the suspension, removing the supernatant solution, and adding fresh water does not accelerate the process thus confirming its irreversibility. This fact resulted in the observation that not only the quantity but also the quality of the loading changed during the displacement.

On the basis of these observations and the consideration of space-filling van der Waals models, we deduced a mechanism for the displacement process (see Scheme 3). As can be seen in Scheme 2, the main channels of zeolite L are made by the stacking of sections with a length of 7.5 Å in the *c*-direction. The sections are joined by shared 12-membered ring windows having a free diameter of 7.1−7.8 Å. These rings make up the narrowest parts of the main channel. The largest free diameter

is about 13 Å and lies midway between the 12-membered rings mentioned above.[29,31] These structural properties are simplified in Scheme 3 by drawing a cylindrical channel. The displacement process can be outlined as follows: In a first step the solvent molecules penetrate into the channel until they find an intercalated resorufin molecule. This process is probably very fast, since the diffusion of the penetrating solvent through the channel is only hindered by other solvent molecules already present. It thereby has to be pointed out that, in an ideal zeolite L, the solvent molecules can only enter the main channels through the windows at both ends and that the investigated solvent molecules are small enough to easily fit through these windows. To further penetrate into the channel, the solvent molecules have now to pass the resorufin molecule. This second step is decisive for the rate of displacement, and its speed will depend on the size of the solvent molecules. After passing the resorufin molecule, the solvent molecules move on until they encounter the next resorufin molecule. All of the above processes of solvent diffusion are reversible, and solvent molecules may also pass a resorufin molecule in the opposite direction and subsequently leave the channel. Most importantly, the second step results in an accumulation of diffusing solvent molecules in the void volume around the resorufin molecule, which leads to the mobilization of the latter. The thereby initiated diffusion of the resorufin molecule will after a certain period of time result in its release into the solution surrounding the zeolite. As pointed out already, the resorufin molecules in solution are deprotonated and will therefore not be able to reenter the zeolite channel. It follows that the rate of the increase of the concentration of Res^- molecules in the solution is a measure for the ability of the solvent molecules to pass the resorufin molecules inside the zeolite main channel.

Modeling of the Exit Kinetics. The diagonal elements m_{kk} of the transition matrix **M** are a measure for the accessibility of the site to entering solvent molecules. The accessibility depends on the position of the site inside the channel and on the amount of resorufin molecules located on both sides and on the site itself, thus shielding it from entering solvent molecules. While the former contribution to the accessibility is independent of time, the latter does change during the displacement process. At this point we must distinguish three cases. In case 1 the solvent molecules can pass a resorufin molecule inside the channel easily, which means that the resorufin concentration inside the channels does not influence the matrix elements and therefore a homogeneous Markoff chain may be applied. In case 2 the process is considerably slowed because the solvent molecules are too large to pass a resorufin molecule easily. Hence, the displacement process is facilitated when the amount of resorufin molecules in the channel is reduced. Case 2 develops into case 3 when the solvent molecules are so large that they cannot pass the resorufin molecules at all.

We now explain the mathematical description of case 1: It is reasonable to assume that the probabilities for a jump to the left and a jump to the right are equal. On the basis of this assumption and eq 6, the off-diagonal elements of **M** can be calculated from the diagonal elements. To determine the transition matrix and thus the Markoff chain, we had to develop a function to calculate the values of m_{kk}. The following Gaussian type function was chosen:

$$m_{kk} = B \exp\left(\frac{-(k-50)^2}{A}\right) \tag{8}$$

The transition matrix is therefore determined by the parameters

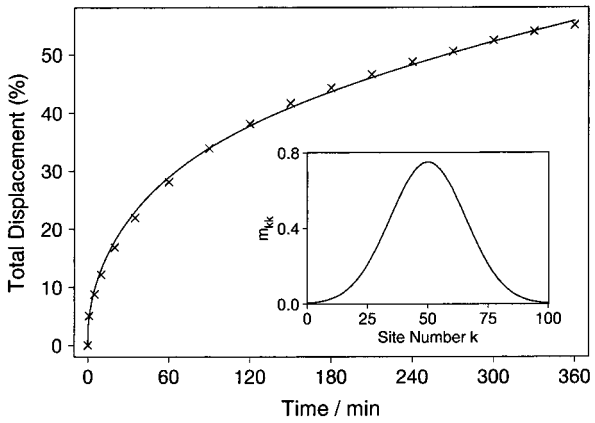

Figure 8. Simulation of the exit kinetics based on the Markoff chain model. The solid line represents the calculated results. Experimental values are shown as crosses. The diagonal elements m_{kk} of the transition matrix were determined by the use of eq 8 with $A = 490$ and $B = 0.75$. The Gaussian distribution of the diagonal elements m_{kk} is illustrated in the insert.

A and B. We finally have to consider the sites at both ends of the channel. It is obvious that the total occupation probability, which is the sum over all p_k-values, has to decrease with time. This is taken into account by setting the probabilities for a jump to the neighboring sites equal to zero at the sites $k = 0$ and $k = 100$. This means that a resorufin molecule reaching one of these two sites will either stay during the next calculation step (this probability is given by $m_{0,0}$ and $m_{100,100}$) or be lost, which apparently means being released into the surrounding solution. The occupation probability of resorufin molecules in solution after s calculation steps can thus be determined as follows:

$$q(s) = 1 - \sum_{k=0}^{100} p_k(s) \tag{9}$$

q(s) corresponds to the increase in concentration of resorufin molecules in solution in proportion to the total amount of resorufin present in the suspension and can therefore be compared with experimental results.

While case 3 describes a stable situation, the kinetics of case 2 depend on specific conditions which lead to inhomogeneous Markoff chains. There is no need in the present study to describe this more complex topic in detail, but we will add some remarks at the end of this section.

We now apply the homogeneous Markoff chain described above to model the exit kinetics in water over a period of 360 min. Therefore, the parameters A and B and the time interval Δt between two calculation steps have to be chosen. It thereby has to be considered that the values of A and B depend on the choice of Δt. Time intervals larger than 10 s do not yield satisfactory results because the number of calculated steps is not sufficient. Time intervals smaller than 0.5 s should equally be avoided since they cause A to get very large, which means that the Gaussian type function determining the values of m_{kk} gets flat and loses its desired features. Choosing $A = 490$ and $B = 0.75$ and calculating 2160 steps ($\Delta t = 10$ s) yields a curve which corresponds very well to the experimental values, as can be seen in Figure 8. The calculated occupation probabilities at different times are shown in Figure 9. Apparently not only the quantity but also the quality of the loading changes during the displacement process. The occupation probability at inner sites increases compared to the sites which are located toward the openings of the channel. This can also be observed experimentally: Resorufin-loaded samples of zeolite L which have

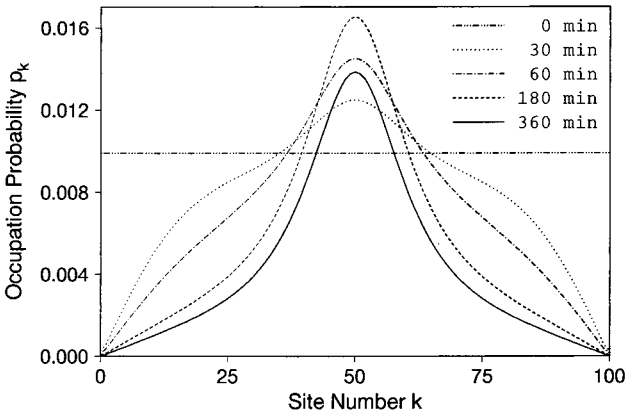

Figure 9. Calculated development of the occupation probabilities p_k according to the simulated displacement process shown in Figure 8.

been shortly exposed to water show slower exit kinetics than samples with a more uniform occupation of the sites.

The solvent molecules apparently play an important role in the displacement process, which can be shown by excluding their influence from the simulation by assuming that the diffusion of the resorufin molecules does not follow a mobilization process initiated by solvent molecules and that they are diffusing freely, regardless of the position of the site on which they are located. This can be done by setting all diagonal elements m_{kk} of the transition matrix to the same constant value somewhere between 0 and 1, which means that according to eq 6 all nonzero off-diagonal elements also have the same value $^1/_2(1 - m_{kk})$. It then can be observed that the displacement process is basically simulated too slow at the beginning and too fast toward the end.

Since we only use one resorufin molecule in our model, interactions between resorufin molecules inside the main channel are not explicitly taken into account. The consequences of this neglect are not significant, because the initial loading of the zeolite samples used for measurement was small: Assuming a homogeneous distribution, there is only one resorufin molecule every 10 sites. By using a homogeneous Markoff chain, we also neglected the shielding of the sites by surrounding resorufin molecules. Since the influence of this shielding effect increases with increasing size of the solvent molecules, it has to be considered when simulating the displacement process in methanol. In this case an inhomogeneous Markoff chain has to be applied. This means that the values of m_{kk} are now different for every single calculation step. The inclusion of an appropriate time dependence into eq 8 requires at least two additional parameters, which renders the mathematical description more complex.

Conclusions

We have presented the intercalation of the anionic organic dye molecule resorufin into the negatively charged channels of zeolite L. The inclusion was attained by incorporating the neutral form of the dye from the gas phase and deprotonating it by exchanging the protons with potassium ions. The remarkably different UV/vis absorption spectra of ResH and Res^-, which we explained with quantum chemical calculations based on the EHMO-EDiT theory, are convenient for distinguishing between the two forms of the dye molecule. The quenching of the fluorescence of the resorufin anion inside the zeolite channels allowed us to study the exit kinetics of the intercalated molecules in the presence of differently sized solvent molecules. For solvent molecules which are small enough to pass the resorufin molecules inside the channel easily, a homogeneous Markoff chain can be used to discuss the exit kinetics. It thereby could be shown that the mobility of the resorufin molecules decreases with increasing distance from the opening of the channels. If the solvent molecules are too large to pass the resorufin molecules inside the channels, no displacement of resorufin can be observed even if it is soluble in the investigated solvent. Solvents with these properties can therefore be used to remove resorufin molecules from the outer surface of the zeolite particles without displacing the intercalated resorufin molecules. We have observed that this procedure is also applicable to methylviologen in zeolite L.[32] Furthermore, the mechanism of displacement according to case 3 is likely to play an important role in experiments with oxonine and methylene blue where solvatochromy can be used to distinguish between molecules at the outer surface and on the inside of zeolite L microcrystals.[7] We therefore expect that the mechanisms of displacement given in this paper can be applied to other cases where molecules in the channels of microporous materials are of interest.

Acknowledgment. This work was supported by the Swiss National Science Foundation Project NF 2000-046617.96/1 and Project NFP 36,4036-043853/1.

References and Notes

(1) Bein, T. *Chem. Mater.* **1996**, *8*, 1636.
(2) Caro, J.; Marlow, F.; Wübbenhorst, M. *Adv. Mater.* **1994**, *6*, 413.
(3) Hoffmann, K.; Marlow, F.; Caro, J. *Adv. Mater.* **1997**, *9*, 567.
(4) Persaud, L.; Bard, A. J.; Campion, A.; Fox, M. A.; Mallouk, T. E.; Webber, S. E.; White, J. M. *J. Am. Chem. Soc.* **1987**, *109*, 7309.
(5) Rolison, D. R. In *Advanced Zeolite Science and Applications, Studies in Surface Science and Catalysis, Vol. 85*; Jansen, J. C., Stöcker, M., Karge, H. G., Weitkamp, J., Eds.; Elsevier: Amsterdam, 1994; p. 543.
(6) Binder, F.; Calzaferri, G.; Gfeller, N. *Sol. Energy Mater. Sol. Cells* **1995**, *38*, 175.
(7) Binder, F.; Calzaferri, G.; Gfeller, N. *Proc. Indian Acad. Sci. (Chem. Sci.)* **1995**, *107*, 753.
(8) Gfeller, N.; Calzaferri, G. *J. Phys. Chem. B* **1997**, *101*, 1396.
(9) Gfeller, N.; Megelski, S.; Calzaferri, G. *J. Phys. Chem. B* **1998**, *102*, 2433.
(10) Jobic, H.; Hahn, K.; Kärger, J.; Bée, M.; Tuel, A.; Noack, M.; Girnus, I.; Kearley, G. J. *J. Phys. Chem. B* **1997**, *101*, 5834.
(11) Barrer, R. M.; Walker, A. J. *Trans. Faraday Soc.* **1964**, *60*, 171.
(12) Calzaferri, G.; Gfeller, N.; Pfanner, K. *J. Photochem. Photobiol. A: Chem.* **1995**, *87*, 81.
(13) Seel, F. *Stud. Inorg. Chem.* **1984**, *5*, 67.
(14) Lindner, G. G.; Reinen, D. *Z. Anorg. Allg. Chem.* **1994**, *620*, 1321.
(15) Calzaferri, G.; Gfeller, N. *J. Phys. Chem.* **1992**, *96*, 3428.
(16) Ramamurthy, V.; Sanderson, D. R.; Eaton, D. F. *J. Am. Chem. Soc.* **1993**, *115*, 10438.
(17) Musso, H.; Rathjen, C. *Chem. Ber.* **1959**, *92*, 751.
(18) Musso, H.; Matthies, H.-G. *Chem. Ber.* **1957**, *90*, 1814.
(19) Eichler, H. *J. Prakt. Chem.* **1934**, *139*, 113.
(20) Calzaferri, G.; Rytz, R.; Brändle, M. *ICON-EDiT, Extended Hückel Molecular Orbital and Transition Dipole Moment Calculations*; available via http://iacrs1.unibe.ch (130.92.11.3), 1997.
(21) Hoffmann, R. *J. Chem. Phys.* **1963**, *39*, 1397.
(22) Wolfsberg, M.; Helmholz, L. *J. Chem. Phys.* **1952**, *20*, 837.
(23) Calzaferri, G.; Forss, L.; Kamber, I. *J. Phys. Chem.* **1989**, *93*, 5366.
(24) Calzaferri, G.; Rytz, R. *J. Phys. Chem.* **1995**, *99*, 12141.
(25) Miller, P. J. *Educ. Chem.* **1972**, *9*, 222.
(26) Formosinho, S. J.; Miguel, M. M. *J. Chem. Educ.* **1979**, *56*, 582.
(27) Schellenberg, P.; Friedrich, J. *J. Lumin.* **1993**, *56*, 143.
(28) Drexhage, K. H. *Laser Focus* **1973**, *9*, 35.
(29) Barrer, R. M.; Villiger, H. *Z. Kristallogr.* **1969**, *128*, 352.
(30) Breck, D. W. *Zeolite Molecular Sieves*; John Wiley & Sons: New York, 1974; p 113 ff.
(31) Meier, W. M.; Olson, D. H.; Baerlocher, Ch. *Atlas of Zeolite Structure Types*; Elsevier: London, 1996.
(32) Hennessy, B.; Marcolli, C.; Megelski, S.; Gfeller, N.; Calzaferri, G. To be published.